B0501

Strontium Titanate based SOFC anodes with nano scaled electrocatalysts

Peter Holtappels (1), Nasima Arshad (2), Daniel Bøgh Drasbæk (1), Nazan Muzaffar(1,2), Bhaskar Reddy Sudireddy (1), Marie Lund Traulsen(1)
(1) Technical University of Denmark, Department of Energy Conversion and Storage
2800 Kgs Lyngby/Denmark
(2) Department of Chemistry, Allama Iqbal Open University, 44000 Islamabad/Pakistan

Contact authors: www.EFCF.com/ContactRequest

Abstract

Ceramic SOFC anodes with nano scaled electrocatalyst particles are of current interest for low temperature application of SOCs and to increase robustness in terms of redox stability and coking tolerance. Strontium titanates are a materials class that is compatible with the state-of the art electrolyte yttria stabilized zirconia and possesses sufficient electronic conductivity under reducing conditions that make them attractive for SOC fuel electrodes. However, their electrocatalytic activity is rather poor and nano scaled electrocatalyst particles are infiltrated into the porous strontium titanate to achieve technically relevant performance. Various electroactive materials have been explored by infiltration into Strontium titanates. Ni, Co and Fe with and without ceria-gadolinia (CGO) have been infiltrated as metal particles into two different Strontium titanates, A-site deficient La-Sr-C-titanate (LSCT) modified with different elements (Cr, Mn, Zn) on the B-site and Niobium modified Strontium-titanate (STN). Zn substitution showed a positive effect on the pure LST electrodes and electrode area specific resistances down to 0.2 $\Omega\cdot cm^2$ have been achieved for LST-Zn electrodes infiltrated with Ni-CGO. The influence of backbone vs. electrocatalyst on the electrode performance will be presented in this contribution.

Introduction

Ceramic SOFC anodes with nano scaled electrocatalyst particles are of current interest for low temperature application of SOCs, and as regards increase in robustness in terms of redox stability and coking tolerance.

Strontium titanates are a materials class that is compatible with the state-of the art electrolyte yttria stabilized zirconia and that possesses sufficient electronic conductivity under reducing conditions, which make them attractive for SOC fuel electrodes (1-5). However, their electrocatalytic activity is rather poor and nano scaled electrocatalyst particles are usually infiltrated into the porous strontium titanate to achieve technically relevant performance. Mostly Ni with or without ceria is infiltrated as electroctalysts, and promising results have been obtained for A and B-site modified strontium titanates including Nb-doped strontium titanate (STN), and La-Ca modified strontium titanate (LSCT) (4-6). However, even if redox stability could be achieved, problems with coking and sulphur poisoning are still a problem and associated with the use of Ni as electrocatalyst (7). Studies comparing different electrocatalysts on STN have been performed as regards their activity and tolerance to coking and exposure to high humidity contents (7-9).The results show clearly that the nature of the electrocatalyst, as well as the presence of CGO positively affects the electrode performance.

To better understand the role of the backbone material as electrocatalyst support on the fuel electrode performance, the variation of the strontium titanate backbone in relation to various electrocatalytically active infiltrates is on focus in the present study.

1. Scientific Approach

The approach is to investigate the electrochemical performance of different backbones and electrocatalysts as regards their electrochemical performance at OCV conditions. Ni, Co and Fe with and without ceria-gadolinia (CGO) have been infiltrated as metal particles into two different strontium titanates, niobium modified strontium-titanate (STN) and Ca modified A-site deficient La-Sr-titanate (LSCT) modified with different elements (Cr, Mn, Zn) on the B-site (LSCTC, LSCTM, LSCTZ, respectively). These elements have compatible ionic radii to Ti-ions, but due to different valence states can affect differently the defect chemistry and electronic properties of the host material.

2. Experiments

The synthesis of $La_{0.2}Sr_{0.25}Ca_{0.45}TiO_3$ (LSCTA) as well as B- site doping on the LSCTA with Zn, Mn and Cr (1%, 5%) was done by the Pechini method using nitrate salts as precursors (10). Stoichiometric amounts of the metals nitrates (Aldrich) were dissolved in an aqueous solution. The solution of ethylene glycol and citric acid (both Sigma-Aldrich) was added with a final molar ratio of metal ions to citric acid to ethylene glycol as 1:4:16. The solution was then heated on hot plate at 80-100 °C, to form the gel and subsequently heated at 300 °C for combustion. The resulting powder was dried and calcined in air for 5 hours at 1200 °C. The phase formation was identified by XRD (Bruker) using Cu-Kα radiation in the range of 20° – 80°.

The doped analogues of LSCTA are denoted LSCTZ1 ($La_{0.2}Sr_{0.25}Ca_{0.45}Ti_{0.99}Zn_{0.01}O_3$) and LSCTZ5 ($La_{0.2}Sr_{0.25}Ca_{0.45}Ti_{0.95}Zn_{0.05}O_3$), LSCTM1 ($La_{0.2}Sr_{0.25}Ca_{0.45}Ti_{0.99}Mn_{0.01}O_3$) and

LSCTM5 ($La_{0.2}Sr_{0.25}Ca_{0.45}Ti_{0.95}Mn_{0.05}O_3$), LSCTC1 ($La_{0.2}Sr_{0.25}Ca_{0.45}Ti_{0.99}Cr_{0.01}O_3$) and LSCTC5 ($La_{0.2}Sr_{0.25}Ca_{0.45}Ti_{0.95}Cr_{0.05}O_3$).

B-site Nb substituted strontium titanate, $Sr_{0.94}Ti_{0.9}Nb_{0.1}O_3$, (STN94), was prepared from $SrCO_3$, TiO_2 and Nb_2O_5 (all materials >99.9 purity, Sigma-Aldrich, Germany) by solid-state reaction method.

For fabrication of the symmetrical cells, STN94 ink was spray deposited onto a pre-sintered 240 ±10 µm thick Sc_2O_3, Y_2O_3 co-stabilized ZrO_2 (Sc-YSZ) electrolyte. After deposition, the electrodes were sintered at 1200 °C for 8h in air, resulting in electrode thicknesses between 20 and 40 µm. A detailed description of the fabrication procedure of the symmetrical cells can be found in (11). After sintering, the cells were laser cut into smaller pieces of 0.6 cm × 0.6 cm.

The infiltration solutions were prepared by dissolving the respective metal nitrates in water along with a surfactant. Metal concentration in the solution was kept to 1M. Prior to infiltration, the symmetrical cells were weighted, and the infiltration was then performed by dropping the nitrate solution onto both porous electrode layers with subsequent heating to 350°C for 30 minutes. This infiltration procedure was repeated three times in total, with the last heat-treatment step at 350°C prolonged to two hours. The thus obtained catalyst loadings are around 0.6 -1 w% (8).

The microstructure of the cells was investigated from a fractured cross-section, without any pretreatment of the samples, using scanning electron microscopy (SEM) (ZEISS Merlin, Carl Zeiss, Germany).

Prior to the electrochemical characterization, the infiltrated cells were hand-painted with a Pt-paste current collection layer. Following this, the cells were mounted in an experimental setup allowing for simultaneous testing of four symmetrical cells per test. A detailed description of the setup can be found elsewhere (12). Cells were investigated by electrochemical impedance spectroscopy at OCV in hydrogen containing 3-4% or 50% water. A Gamry Reference 600 potentiostat was used and impedance spectra were recorded between 0.01Hz-1MHz with 10 points/decade applying a 50 mV amplitude.

Analysis of the impedance data was performed using the Python-based software RAVDAV developed at DTU Energy (13). The series resistances (Rs,) observed in the impedance data were not corrected for ohmic contributions arising from the Pt leads in the experimental setup, as the lead resistance based on previous experiments is estimated to be less than 5% of the measured ohmic resistance (Rs).

3. Results

Figure 1 shows the X-ray diffractograms for LSCT with and without modification by Cr, Mn and Zn. The main phase is the expected perovskite, however small impurity amounts LaO_2, TiO_2 have been observed, varying slightly with composition. The shift to higher 2θ angles for all additions (e.g. visible in the peak at 30° 2θ) suggests a slight reduction of the lattice parameter. The reduction, however, is higher for 1% than for 5% of Cr, almost similar for 1% or 5% Mn, while for Zn additions the lattice gets more reduced with increasing the Zn content from 1% to 5%.
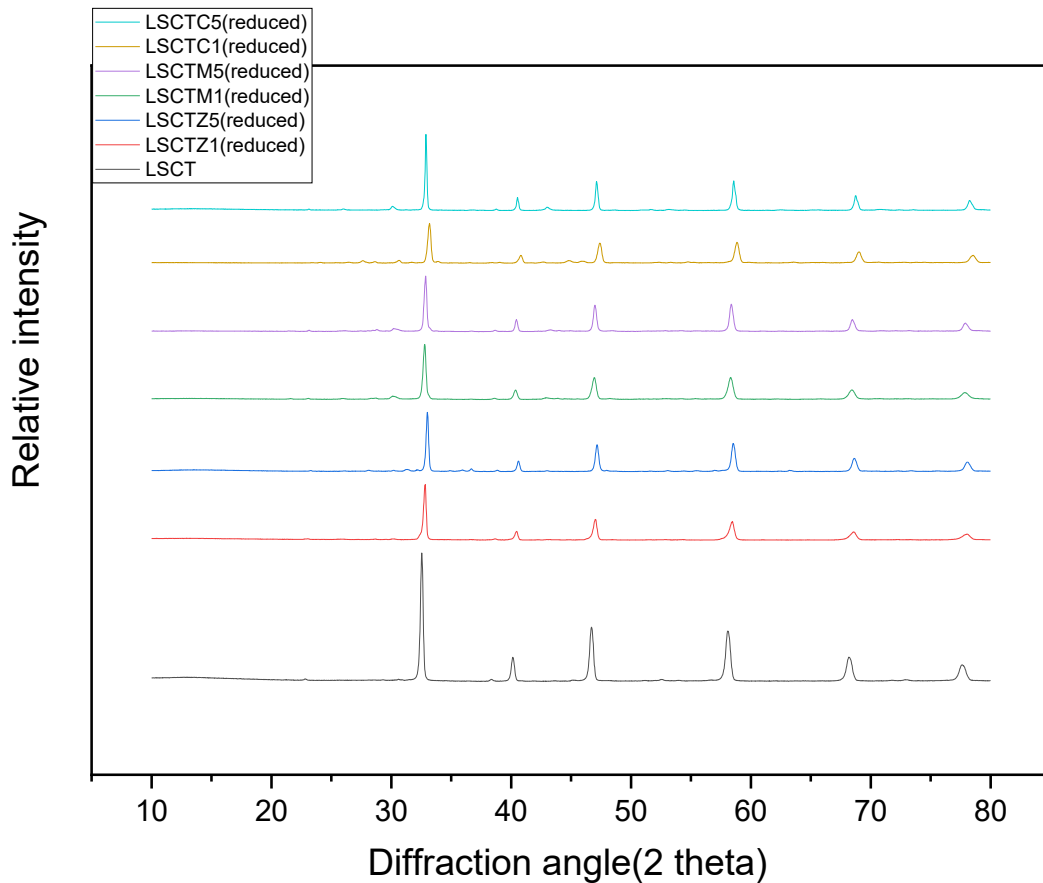
Figure 1   X-ray diffractogramms for LSCT, LSCTM, LSCTC and LSCTZ.

The porous electrode structure is shown in Figure 2 for LSCT with 1% and 5% Zn and shows a well adhering electrode/ electrolyte interface. The electrode microstructures are similar with pore and particle sizes of around 1 micron, which are slightly higher than the pore and particle sizes in STN94 electrodes (8).
Similar adhering electrode structures are obtained for Mn modified LSCT, while crack formation into the electrolyte was observed for Cr modified LSCT. This indicates differences in the sintering behavior of the various modified LSCT, which needs to be further investigated.
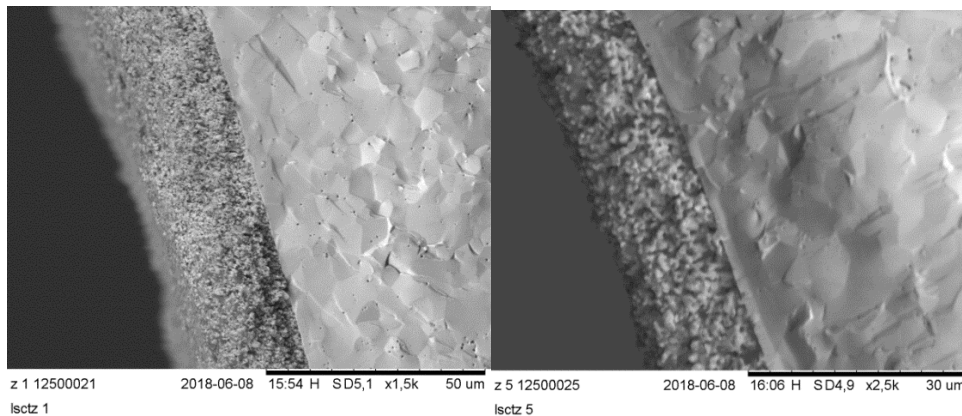

Figure 2   Electrolyte / electrode fracture cross section for LSCTZ1 (left) and LSCT5 (right) electrodes

The dispersion of the infiltrated electrocatalyst into the LSCTZ5 porous electrode backbone can be estimated from Figure 3. The electrocatalysts are evenly distributed and particle sizes are below 100 nm for Ni particles, while slightly larger particles are indicated for Co and Fe. These infiltrate structure are comparable to similar elements infiltrated into STN94 electrodes (8).
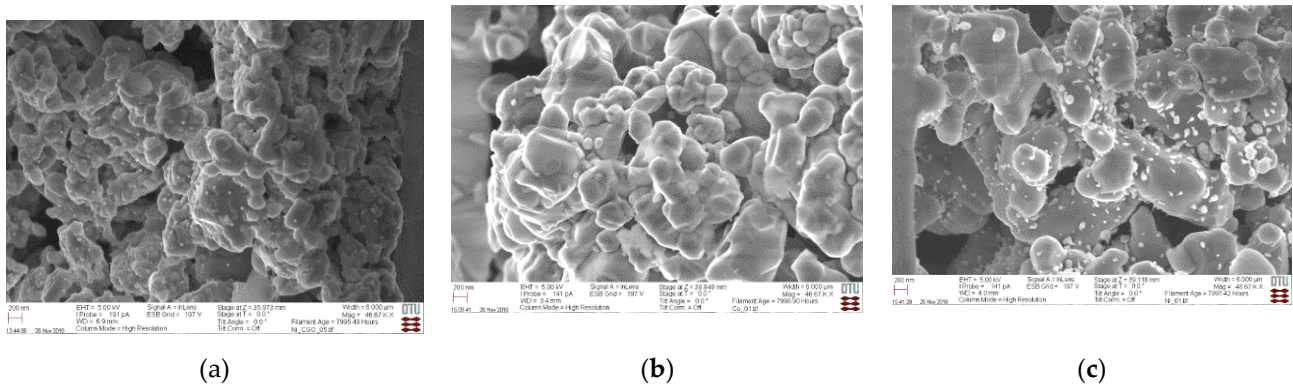

(a)   (b)   (c)

Figure 3   Cross-sectional micrographs of infiltrated symmetrical cells of LSCTZ5 after testing: (a) Ni-CGO infiltrated LSCTZ5, (b) Co-infiltrated LSCTZ5, (c) Fe-infiltrated LSCTZ5. (extracted from (14))

The impedance spectra for the non-infiltrated modified LSCTZ, LSCTC and LSCTM electrodes obtained at open circuit voltage and in hydrogen humidified with 4% water, are presented in Figure 4 for two sintering temperatures 1200 °C and 1250 °C. The higher sintering temperature leads to generally lower faradaic electrode resistances. However, the non symmetrical shape, different for the various modifications, point to different backbone activities. The faradaic electrode resistances for LSCTZ5 are with 25 to 30 Ωcm^2 slightly lower than those presented for STN94. However, a further activation by electrocatalyst addition is clearly needed to reach technically relevant performance.

The temperature dependence of the faradaic electrode resistance is provided in Table 4. Differences between the impedance spectra in Figure 4 and in the activation energies for the modified LSCT electrodes, indicate that the pure ceramic electrode performance is sensitive to composition, fabrication, and testing conditions.
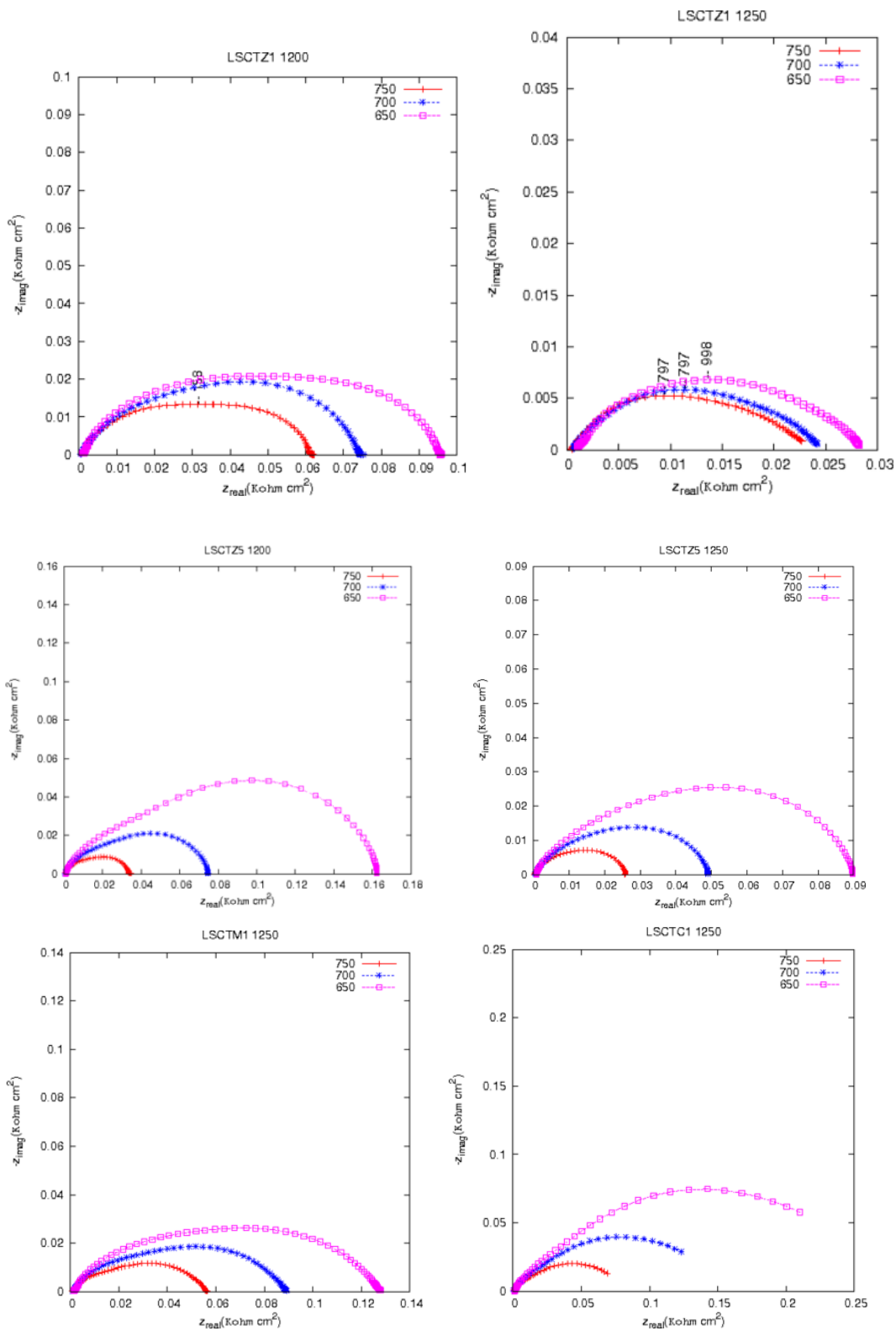
Figure 4   non-infiltrated LSCT electrodes in hydrogen humidified with 4% H_2O for Zn, Mn and Cr modified LSCT sintered at 1200 °C and 1250 °C.

Table 4   Activation energy of the faradaic electrode resistance for the modified LSCT electrodes at OCV.

Samples	Ea (4% H_2O/ H_2)	
	($kJmol^{-1}$)	(eV)
LSCTZ1(1200)	33.42±1.196	0.346±1.196
LSCTZ1(1250)	14.21±0.504	0.147±0.504
LSCTZ5(1200)	124.37±0.527	1.29±0.527
LSCTZ5(1250)	98.43±0.489	1.02±0.489
LSCTM1(1200)	131.69±0.48	1.36±0.48
LSCTM1(1250)	33.58±0.35	0.34±0.35
LSCTC1(1200)	113.9±1.09	1.18±1.09
LSCTC1(1250)	97.52±0.54	1.01±0.54

The faradaic electrode resistances for Ni-CGO, Fe and Co infiltrated LSCTZ5 electrodes is provided in Figure 5 for two different water contents. Increasing the water content lowers the faradaic electrode resistance in case of Co, while it is significantly increased for Fe. As expected, co-infiltrated Ni-CGO shows the lowest faradaic electrode resistance with and decreases similar to Co with increasing water content. This behavior is similar to results on Ni, Co and Fe infiltrated STN94 electrodes (Figure 6). The low faradaic electrode resistance of Ni-CGO infiltrated LSCTZ5 of 0.2 Ωcm^2 at 650°C makes this electrode interesting for low temperature solid oxide fuel cells (14).
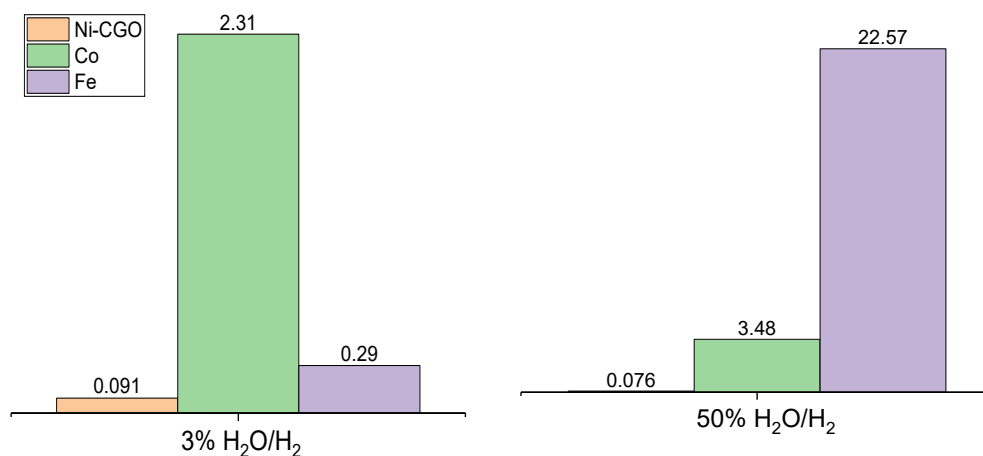

Figure 5   Faradaic electrode resistance for symmetrical LSCT electrodes infiltrated with Co, Fe and Ni-CGO at 750°C in hydrogen humidified with 3-4% water (left) and 50% water (right).

Figure 5 shows the influence of several metallic element infiltration into a STN94 electrode. While infiltration of Mo and W might be interesting in terms of sulphur tolerance,

a poor performance is observed at high water contents. Cu has been discussed as an anode material for direct hydrocarbon conversion, however the electrochemical performance is still inferior to Ni and Co infiltrated cells.
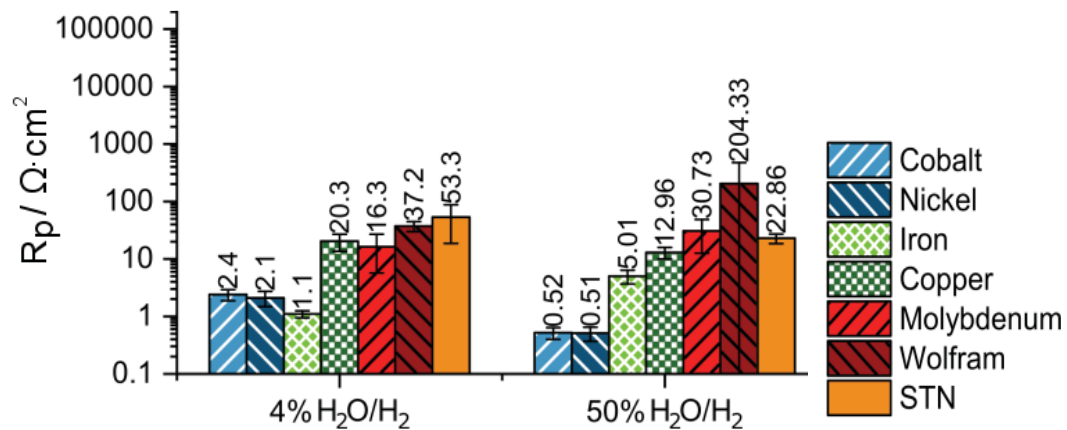

Figure 6   Initial faradaic resistances of metal infiltrated STN94 electrodes at 750°C in humidified hydrogen at OCV

The temperature dependence of the electrode reaction is given in Table 2 for the various infiltrated strontium titanate electrodes. A common trend is that increasing the water content and thus the oxygen partial pressure increases the apparent activation energies of the hydrogen water reaction. For metal only infiltrated electrodes, lower activation energies are observed in all cases for STN94 compared to LSCTZ5, indicating that both, the electrocatalyst and the backbone material are participating in the electrode reaction. Thus, tailoring both, infiltrate and backbone composition, can be utilized to optimize further the electrochemical performance for SOFC anodes.

Table 2   Activation energies of LSCTZ5 and STN94 backbone and infiltrated anodes.

Samples	Activation energy(eV)*	
	(3-4% H_2O/ H_2)	(50% H_2O/ H_2)
LSCTZ5	**1.02**	**-**
STN94	1.06	1.27
LSCTZ5/Ni-CGO	**0.87**	**1.15**
STN94/Ni-CGO	0.68	1.01
LSCTZ5/Co	**1.20**	**1.59**
STN94/Co	0.96	1.48
LSCTZ5/Fe	**0.85**	**1.54**
STN94/Fe	1.52	1.89
*apparent activation energy, as likely not related to a single process		

Acknowledgment

References

[1] A. M. Hussain, J.V.T. Høgh, W. Zhang, N. Bonanos, Efficient ceramic anodes infiltrated with binary and ternary electrocatalysts for SOFCs operating at low temperatures, Journal of Power Sources. 2012, 216.

[2] T. Ramos, C. Bernuy-Lopez, B. R. Sudireddy, J. J. Bentzen, W. Zhang, P. S. Jørgensen, L. T. Kuhn, Performance-Microstructure Relations in Ni/CGO Infiltrated Nb-doped SrTiO3 SOFC Anodes. ECS Transactions. 2012, 45 (1).

[3] P. Blennow, K. K. Hansen, L. R. Wallenberg, M. Mogensen. Electrochemical characterization and redox behavior of Nb-doped SrTIO3, Solid State Ionics. 2009, 180.

[4] M. C. Verbraeken, B. Iwanschitz, A. Mai, J.T.S. Irvine, Evaluation of Ca Doped La0.2Sr0.7TiO3 as an Alternative Material for Use in SOFC Anodes, J. Electrochem. Soc., 2012, 159(11).

[5] Q. Ma, F. Tietz, A. Leonide, E. Ivers-Tiffée, Electrochemical performances of solid oxide fuel cells based on Y-substituted SrTiO3 ceramic anode materials, J. Power Sources. 2011, 196.

[6] T. Ramos, S. Veltzé, B. R. Sudireddy, P. S. Jørgensen, L. Theil Kuhn, P. Holtappels. Effect of Ru/CGO versus Ni/CGO Co-Infiltration on the Performance and Stability of STN-Based SOFCs, Fuel Cells 14. 2014, 6.

[7] D. B. Drasbæk, M. L. Traulsen, R. A.Walker, P. Holtappels, Testing Novel Nickel and Cobalt Infiltrated STN Anodes for Carbon Tolerance using In Situ Raman Spectroscopy and Electrochemical Impedance Spectroscopy, FUEL CELLS 19, 2019, No. 4, 484–493

[8] D.B. Drasbæk, M.L. Traulsen, B.R. Sudireddy, P.Holtappels, Understanding the Electrocatalytic Activity of Transition Metal Nanoparticles for Solid Oxide Cell Fuel Electrodes, Electrochimica Acta 327 (2019) 135004

[9] D.B. Drasbæk, M.L. Traulsen, B.R. Sudireddy, P. Holtappels, Combining Transition Metals – An approach towards High-performing Coking Tolerant Solid Oxide Fuel Cell Anodes, ECS Transactions, 91 (1) (2019) 1953-1961.

[10] C.D. Savaniu, D.N. Miller, J.T.S Irvine, Scale up and anode development for La-Doped SrTiO3 anode-supported SOFCs, J. Am. Ceram. Soc. 2013, 96, 1718–1723.

[11] T. Ramos, C. Bernuy-Lopez, B. R. Sudireddy, J. J. Bentzen, W. Zhang, P. S. Jørgensen, L. T. Kuhn, Performance-Microstructure Relations in Ni/CGO Infiltrated Nb-doped $SrTiO_3$ SOFC Anodes, ECS Transactions. 2012, 45 (1)

[12] T. Ramos, K. Thyden, M. Mogensen, Electrochemical characterization of Ni/(Sc) YSZ electrodes, ECS Transaction 28 (2010) https://doi.org/10.1149/1.3495837

[13] Chris Graves, RAVDAV Data Analysis Software, DTU, 2015, version 0.9.8

[14] N. Muzaffar, N. Arshad, D.B. Drasbæ, B.R. Sudireddy, P. Holtappels, Fabrication and Electrochemical Performance of Zn-Doped $La_{0.2}Sr_{0.25}Ca_{0.45}TiO_3$, Infiltrated with Nickel-CGO, Iron, and Cobalt as an Alternative Anode Material for Solid Oxide Fuel Cells, Catalysts 2019, 9, 269